JCBPS; Section A; May 2018 – July - 2018, Vol. 8, No. 3; 325-343. E- ISSN: 2249 –1929
[DOI: 10.24214/jcbps.A.8.3.32543]

Journal of Chemical, Biological and Physical Sciences

An International Peer Review E-3 Journal of Sciences

*Available online at*www.jcbsc.org

Section A: Chemical Sciences

CODEN (USA): JCBPAT Research Article

Influence of *Punica Granatum* plant extract on corrosion of aluminum in 1 M HCl

A.S.Fouda[1], Shady M. El – Dafrawy[1], Ali M. El-Azaly [2] and Eslam S. El-hussieny[2]

[1] Department of Chemistry, Faculty of Science, El-Mansoura University, El-Mansoura-35516, Egypt

[2] Department of Chemistry, Faculty of Engineering, Nile higher institute for engineering, Mansoura, Egypt

Received: 20 April 2018; **Revised:** 05 May 2018; **Accepted:** 11 May 2018

Abstract: Punica Granatum Extract (PGE) is a corrosion inhibitor used for Al alloy in 1.0 M HCl solution utilizing weight loss (WL), Tafel polarization (PP), electrochemical impedance spectroscopy (EIS) and electrochemical frequency modulation (EFM) techniques. A scanning electron microscope (SEM) has utilized to determine the surface morphology for Al. The temperature influence on corrosion performance with the appending of several doses was considered in the range of 25-45 ºC by WL. PP diagrams illustrate that PGE is a mixed inhibitor. The protection efficiency (IE), increased by increasing PGE concentration and with increasing temperature of solution. Temkin's adsorption isotherm was found to be the suitable isotherm to express adsorption of the extract on surface of Al. The activation and adsorption parameters had measured and discussed. Chemical and electrochemical techniques were utilized to get results which were found to be in good agreement.

Keywords: HCl, Aluminum alloy, PGE, Corrosion inhibition, EIS, EFM, SEM.

INTRODUCTION

The corrosion process is considered a fundamental process, which plays a vital character in safety and economics, especially for metals. The best one test for hindrance versus corrosion is the use of inhibitors, exclusively in acidic media[1]. Nitrogen , sulfur, and oxygen atoms which are found in organic compounds are considered to act as inhibitors. These inhibitors got a lot of advantages such as easy production and high inhibition efficiency[2-5]. For the corrosion inhibition of aluminum[6-8], organic heterocyclic compounds have been used as well as for copper[9], iron[10-13] and other metals[14-15] in various corrosive media. Though a lot of these organic heterocyclic compounds have great protection efficiencies, many of them have unwanted side effects, until if they are in minor doses, because their toxicity to the environment or humans, besides being expensive[16]. Economical and safe environment is the chief advantages for utilizing extracts as corrosion protection. Thus far, numerous extracts have been utilized as corrosion hindrance for Al in acidic solution, for instance: Garlic, Black Mulberry, piper Guineans seed and Red onion skin[17-20]. Punica Granatum extract (PGE) common name is pomegranate and it belongs to the family Lythraceae. This extract can act as an actual combat tool, versus heart sickness, in effect detoxifying agent, higher source of vitamin c, dental hygiene, for cough, sore throats, for healthy hair and skin, effective moisturizer[21].

2. MATERIAL AND METHODS

2.1. Materials and solutions: The chemical conformation of utilized Al (% weight) is Fe 0.60, Si 0.30, Mg 0.05, 1.40 Mn, 0.100 Cu, 05 Ti, 0.05 Cr and the rest is Al. The Pt wire (1 cm^2), while (SCE) connected to an electrolytic cell of capacity 100 ml via a bridge with a Luggin capillary. Preparation of corrosive reagent grade, 34% HCl with bi-distilled water was made for preparation of the aggressive solution. A PGE (1000 ppm) stock solution was used in order to prepare the required concentrations. PGE concentrations used were 50,100,150,200,250.300 ppm.

2.2. PGE Preparation: A fine powder as prepared by crushing fresh aerial parts of PGE sample. The powdered materials about 250 g were immersed for 5 days in 500 ml dichloromethane and after that imperiled to recurrent removal with 5 x 50 ml until extract plant materials. After dichloromethane was evaporated, a solid extract was obtained, then prepared to be applied as corrosion hindrance. Several analyses have illustrated that the main chemical constituents of PGE are quercetin, Luteolin, gallagic, kaempferol, glycosides, punicalin, punicalagin, pedunculagin[22] as shown in **Figure 1**.

2.3. Measurements of WL: Seven equivalent Al coins of 2x2x0.2 cm were polished with emery papers (grade 340-600-12000 then washed using acetone and bi-distilled water. The immersion of the specimens was taking place in a beaker 250 ml, which enclosed 100 ml HCl existence and nonexistence of containing PGE in different concentrations, after accurate weighing. The grade of (IE %) and surface coverage (θ) of PGE were measured as shown[23] in equation 1:

$$IE\% = \theta \text{ x } 100 = \left[1 - \frac{W}{W^o}\right] x\ 100 \qquad (1)$$

Where, the values of the average weight losses are expressed by W and W^o with and without adding the inhibitor, in that order.

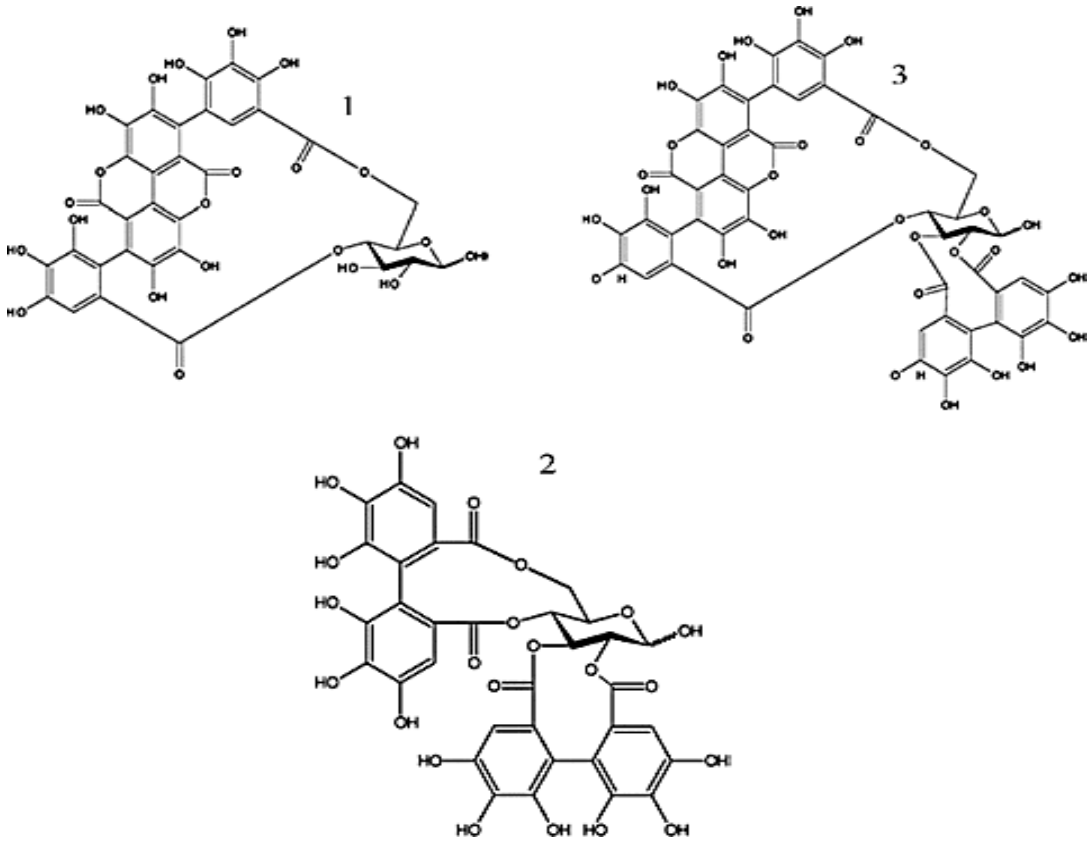

Figure 1: Principal ETs found in the peel of pomegranate. 1: punicalin, 2: pedunculagin, 3: punicalagin

2.4. Electrochemical Techniques

2.4.1. Tafel polarization (PP): Electrochemical tests were accomplished utilizing a distinctive three-compartment glass cell consisting of the Al coins as working electrode (WE) (1 cm^2), a reference electrode like (SCE) and counter electrode (Pt). Under unstirred conditions, all the tests were occurring in solutions (open system). Before each experiment, all potential data were recorded versus SCE, emery paper with successive different grades were used in order to abrade the electrode, then the electrode was degreased using acetone, washed using water bi-distilled and lastly dried. For the calculate of corrosion current, Stern-Geary test[24]] was carried out by anodic and cathodic line extrapolation of data which give (log i_{corr}) and give (E_{corr}) which express the equivalent corrosion potential for hindrance free acid and for each dose of P.G.E.. Then (i_{corr}) was utilized for determination of surface coverage (θ) and (IE %) as in the next equation 2:

$$IE\% = \theta \text{ x } 100 = \left[1 - \frac{i_{corr(inh)}}{i_{corr(free)}}\right] x\ 100 \qquad (2)$$

Where, the corrosion current densities are expressed by $i_{(corr(free))}$ and $i_{(corr(inh))}$ without and with of inhibitor, in that order.

2.4.2. EIS tests: By using AC signals, impedance measurements were accomplished in a range of (2x104 Hz to 8x10-2 Hz) frequencies with 10 mV peak to peak amplitude at OCP. Based on the equivalent circuit, the impedance was examined and explained. R_{ct} that signifies the resistance charge transfer and C_{dl} which signifies the capacity of double layer are both the main parameters realized from the Nyquist diagram analysis. The parameter data gotten from the calculate of impedance is measured from equation 3 as follows:

$$IE\% = \theta \text{ x } 100 = \left[1 - \frac{R_{ct}^{o}}{R_{ct}}\right] x\ 100 \qquad (3)$$

Where, the charge transfer resistance is expressed by R_{ct}^{o} and R_{ct} without and with inhibitor, in that order.

2.4.3. EFM tests: EFM was accomplished by using two frequencies (2 and 5 Hz). The waveform repeats after 1 s, because 0.1 Hz represented the base frequency. The lower frequency must be no more than half the higher one. The greater frequency must be adequately slow, so the double layer charging does not contribute to the response current. Often, the reasonable limit is about 10 Hz. Harmonic and intermodulation current peaks illustrated current responses in the intermodulation spectra. (i_{corr}) which represents the corrosion current density, (β_a and β_c) which represent[25] the Tafel slopes and CF-2 & CF-3 which represent the causality factors were computed using the large peaks. In 30 min before the beginning of the measurements, stabilization of the electrode potential was allowed. At 25°C, all the experiments were conducted. By using the instrument of Gamry (PCI4/750) Potentiostat/Galvanostat/ZRA, all electrochemical measurements were carried out. Gamry requests contain DC105, EIS 300 software and EFM 140 software for PP, EIS and EFM tests by collecting data via computer, respectively. For drawing, graphing and fitting data, Echem 6.03 software were used.

2.5. Study of Al surface morphology: About morphological study, features of the Al alloy surface was examined using the SEM JEOL JSM-5500 beforehand and afterward inundation in 1.0 M HCl solution for 24 hour with and without P.G.E.

RESULTS AND DISCUSSION

3.1. WL tests: In the absence and presence of different doses of PGE WL tests were done for Al in 1.0 M HCl and are displayed in Figure (2). We listed the measured data of %IE in table (1). From these tables, it is noted that IE% is directly proportional to the concentration of PGE and inversely proportional to the temperature rising from 25-45°C. The detected PGE inhibition action could be referred to its components' adsorption on the surface of Al. The adsorbed molecules forms a layer which isolates the aggressive medium away from the surface of Al by blocking the corrosion centers on the surface which limits the medium liquefaction and then the corrosion rate decreases, by improving efficiency as their concentrations rise[26].

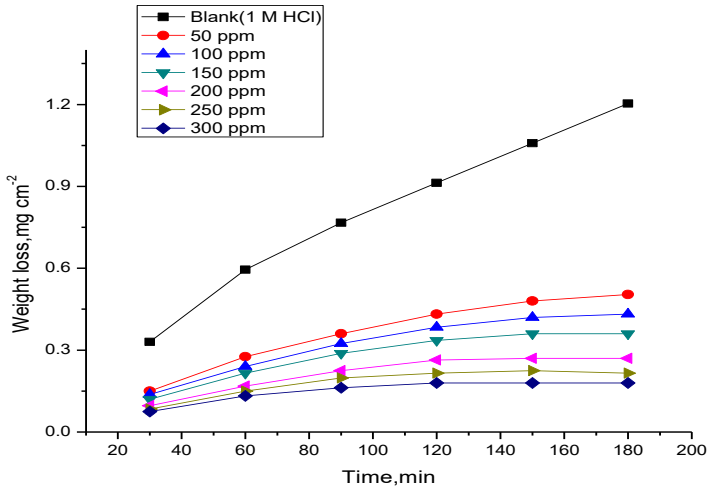

Figure 2: WL - time curves for Al corrosion in 1 M HCl in the presence and absence of PGE at 25°C

Table 1: (k_{corr}) is corrosion rate, (Θ) is surface coverage and (IE%) is an inhibition efficiency variation with different concentrations of PGE immersed in M HCl at different temperatures after 120 minutes.

Temperature in °C.	[Inh]. ppm	Weight loss, mg cm^{-2}	k_{corr}, mg cm^{-2} min^{-1}	Θ	%I.E
25	Blank	0.91	0.0076	-	-
	50	0.43	0.0036	0.5267	52.67
	100	0.38	0.0032	0.5793	57.93
	150	0.34	0.0028	0.6319	63.19
	200	0.26	0.0022	0.7107	71.07
	250	0.22	0.0018	0.7633	76.33
	300	0.18	0.0015	0.8082	80.82
30	Blank	2.48	0.021	-	-
	50	1.27	0.011	0.4866	48.66
	100	1.10	0.009	0.5584	55.84
	150	0.99	0.008	0.5998	59.98
	200	0.78	0.007	0.6849	68.49
	250	0.62	0.0052	0.7493	74.93
	300	0.55	0.0046	0.7767	77.67
35	Blank	6.35	0.054	---	---
	50	3.63	0.030	0.4445	44.45
	100	3.02	0.025	0..5372	53.72
	150	2.83	0.024	0.5662	56.62
	200	2.23	0.019	0.6578	65.78
	250	1.73	0.0144	0.7350	73.50
	300	1.64	0.0137	0.7483	74.83

40	Blank	16.65	0.139	---	---
	50	9.98	0.083	0.4005	40.05
	100	8.76	0.073	0.4739	47.39
	150	7.52	0.063	0.5483	54.83
	200	6.17	0.051	0.6293	62.93
	250	4.66	0.039	0.7204	72.04
	300	3.93	0.033	0.7641	76.41
45	Blank	41.26	0.344	----	---
	50	26.36	0.222	0.3546	35.46
	100	23.28	0.194	0.4358	43.58
	150	19.87	0.166	0.5184	51.84
	200	16.53	0.138	0.5994	59.94
	250	12.15	0.101	0.7054	70.54
	300	10.29	0.086	0.7505	75.05

3.2. PP tests: Figure 3 shows the curves of PP verified for Al in 1 M HCl solution with and without a numerous dose of PGE at 25ºC. Lee and Nobe[27] reported that during potential sweep experiments, a current peak occurred between limiting-current regions and the apparent-Tafel. A remarkable decreasing in the rate of corrosion happens due to the existence of PGE in 1 M HCl, which shifts both the cathodic and anodic branches to the lesser data of the current densities of corrosion. From the PP diagrams in **Figure 3**, the derived parameters are obtained in **Table 2.** The Tafel slopes β_a and β_c at 25ºC do not change remarkably with the presence of PGE, which shows the existence of PGE. Generally, in case of inhibitor presence, if the shift of corrosion potential is less than 85 mV with esteem to that in case of the inhibitor absence, then the classification of the inhibitor can be a mixed kind[28-29]. In our study E_{corr} changes about (20-30 mV) which is very small, this illustrates that PGE can acts as a mixed kind inhibitor.

Table 2: PP parameters for corrosion of Al alloy in 1 M HCl at 25ºC

Inhibitor	[Inh] ppm	$-E_{corr}$ mV vs SCE	i_{corr} mA cm^{-2}	β_a mV dec^{-1}	β_c mV dec^{-1}	CRx10^3 mpy	Ɵ	IE%
Blank	0	725	275	250	420	164	---	---
PGE	50	760	136	150	170	58	0.505	50.5
	100	730	127	80	100	57	0.538	53.8
	150	732	82	60	100	37	0.700	70.0
	200	743	62	30	90	10	0.773	77.3
	250	742	56	20	90	5.3	0.796	79.6
	300	744	30	30	90	5	0.889	88.9

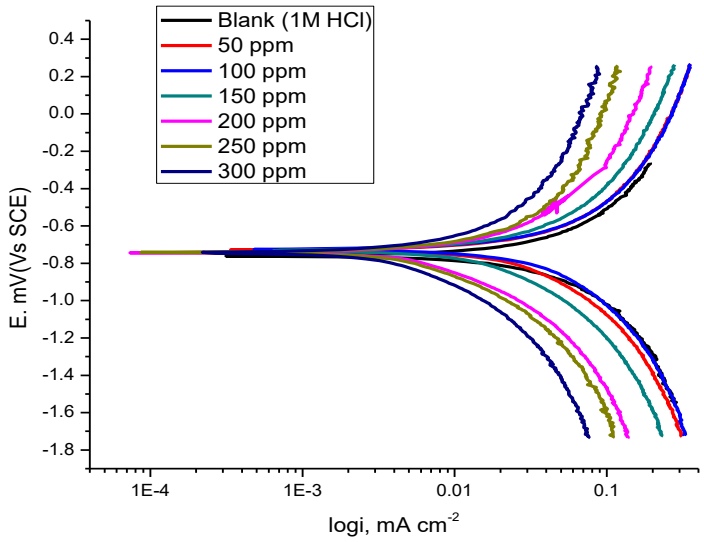

Figure 3: Curves of PP for the Al corrosion in 1 M HCl solution without and with different concentrations of PGE. at 25ºC

3.3. EIS: Impedance plots for Al alloy in 1M HCl solution with and without various doses of PGE are shown in **Figure 4.** A Nyquist semicircle type was found in the impedance spectra without attendance of diffusive influence to the total impedance (Z), signifying that the existence of inhibitor do not change the corrosion reaction mechanism and undergoes mainly under charge-transfer. Due to the frequency dispersion, it was found that there was not a perfect semicircle obtained from Nyquist plots and this behavior due to the roughness[30-31] of the electrode surface. Constant phase element (CPE) is considered as the most widely employed. In universal, a CPE is utilized in a model in order to replace a capacitor to make up for the system[32]. It was established that the semicircle diameters are directly proportional to the concentration of PGE. This illustrates that the thickness of the adsorbed layer increases with increasing PGE concentration and the down capacitive semicircle are regularly attributed to surface inhomogeneity and roughness, since this capacitive semicircle is correlated with the barrier film thickness and dielectric properties[33]. The value illustrated that, each EIS diagram contains a great capacitive loop with frequency dispersion in low values (inductive arc). Generally, this inductive arc referred to anodic adsorbed intermediates controlling the anodic procedure[34, 35].

Figure 5 shows the equivalent electrical circuit model which was utilized for analyzing the obtained impedance data. This model includes the (R_{ct}), (R_s) and the constant phase angle element (CPE). (n) Which is the frequency power data of CPE, can be supposed to parallel to capacitive performance. The permission of CPE is designated in equation 4 as follows:

$$Y_{CPE} = Y_o(j\omega)^n \qquad (4)$$

Where Y_o is the magnitude, J is the imagined root, ω is the angular frequency and n is the exponential term[36].

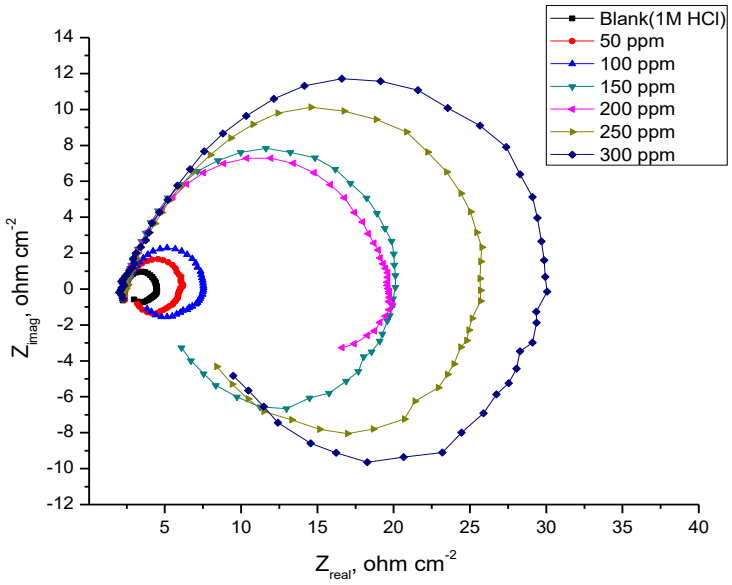

Figure 4: Nyquist plots of Al in 1 M HCl solution with and without different doses of PGE at 25°C

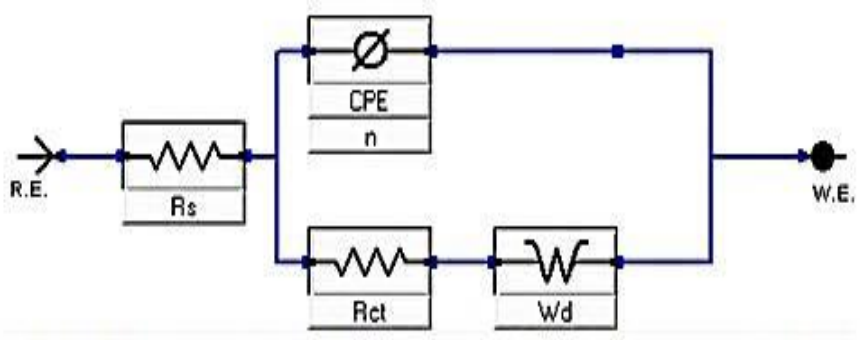

Figure 5: Equivalent circuit used to model impedance data for Al in 1 M HCl Solution

Studies reported in the literature[37] showed that the income data on the corrosion performance of Al in presence the as well as in the absence of PGE have affected by mass transport. In addition, Bode diagrams for the Al in 1M HCl solution have displayed in figure 6. In which R_Ω is a great frequency limit corresponding to the electrolyte resistance while the low frequency signifies the summation of ($R_\Omega + R_{ct}$), where R_{ct} is in the first estimate measure by both electrolytic conductance of the oxide film.

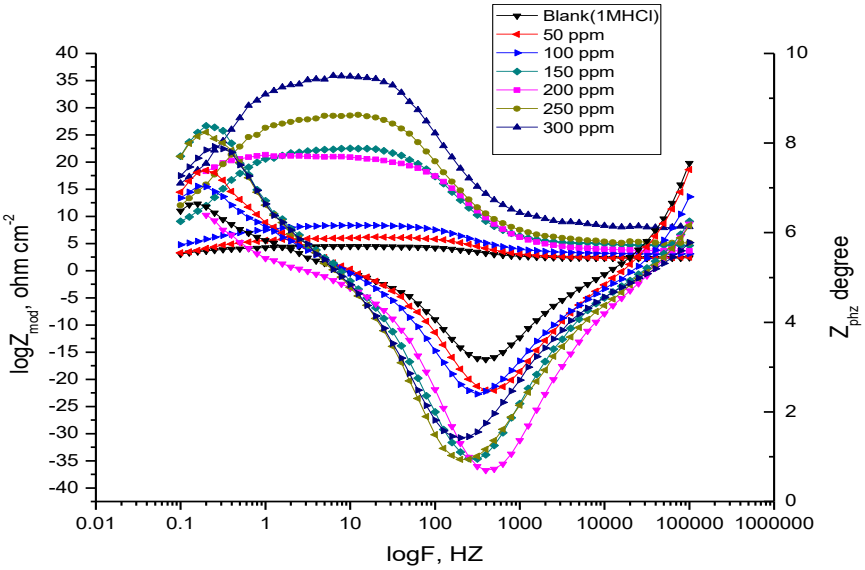

Figure 6: Bode plots for Al in 1 M HCl solution in the presence and absence of different PGE concentrations at 25°C

From the Nyquist diagram analysis, we deduced the following main parameters:

- R_{ct} which represents The charge transfer resistance (high frequency loop diameter)
- C_{dl} which represents The double layer capacity and defined as:

$$C_{dl} = \frac{1}{2\pi R_{ct} f_{max}} \qquad (5)$$

Where f_{max} is the extreme frequency at which the Z_{imag} of a maximum EIS.

Since $\frac{1}{R_{ct}}$ is directly proportional to C_{dl} (Double layer capacity) according to the electrochemical theory, the (IE%) of inhibition of Al alloy in 1 M HCl solution was measured from R_{ct} data which are given by the impedance value at various concentrations of the used inhibitor as the next:

$$\%IE = \left(1 - \frac{R_{ct}^{o}}{R_{ct}}\right) x\ 100 \qquad (6)$$

Where, charge transfer resistance is expressed by R_{ct}^{o} and R_{ct} in the without and with of PGE in that order. From **Table 3** which gives the impedance data, we can conclude that R_{ct} value is directly proportional to the concentration of PGE and this indicates that a passive film was formed on the Al alloy surface by the adsorption, which lead to a rise in the corrosion protection efficiency in HCl solution. While the data of C_{dl} is inversely proportional to PGE concentrations compared to that of blank solution, due to exchange water molecules by PGE, which lead to an improve in the thickness of the formed electric double layer on the Al surface and/or lower in local dielectric constant[38,39].

Table 3: parameters gotten from EIS tests for Al in 1 M HCl without and with various dose of PGE at 25°C

Inhibitor	[Inh] ppm	R_{ct} Ω Cm^2	C_{dl} x 10^6 F Cm^{-2} µ	Θ	%IE
Blank	0	1.7	21	---	---
PGE	50	2.9	5.9	0.468	46.8
	100	3.2	4.4	0.595	59.5
	150	4.2	3.2	0.730	73.0
	200	6.3	3.0	0.760	76.0
	250	7.1	2.5	0.840	84.0
	300	10.9	2.3	0.844	84.4

3.4. EFM tests: EFM is considered as a nondestructive test for corrosion measurement which can calculate the corrosion current value straight away with a small polarizing signal only and without earlier knowledge of Tafel slopes, which makes it a helpful method for online corrosion control[40]. The causality factors are considered as the main advantage of EFM because they act as an internal check on EFM measurement validity. The frequency spectrum of the current responses used in the calculation of the causality factors CF-2 andCF-3. The EFM of Al in 1 M HCl solution including P.G.E at 25°C is displayed in Figure 7. The intermodulation and harmonic peaks are much greater than the background noise and clearly visible. The obtained EFM data were treated for the activation model, supposing that the corrosion potential does not interchange due to the polarization of WE, a set of three non-linear equations had been resolved[41]. The current of corrosion (i_{corr}), (β_c and β_a) which represent the Tafel slops and (CF-2 and CF-3) which represents the causality factors were calculated by the larger peaks. Gamry EFM 140 software was used to simultaneously determine these parameters and recorded in Table 4 showing that P.G.E hindrance the Al corrosion in 1 M HCl with adsorption. Under altered experimental conditions, the obtained CF is nearly equal to (2 and 3) which represent the theoretical values, meaning that the calculated data are in excellent quality and verified[42]. IE_{EFM}%, which represents the inhibitor efficiency is directly proportional to PGE concentrations and was calculated as follows:

$$IE\%_{EFM} = \left[1 - \frac{i_{corr}}{i^o{}_{corr}}\right] x\ 100 \qquad (7)$$

Where, the corrosion current densities are expressed by $i^o{}_{corr}$ and i_{corr} in without and with PGE, in that order.

$$IE\%_{EFM} = \left[1 - \frac{i_{corr}}{i^o{}_{corr}}\right] x\ 100 \qquad (7)$$

Where, the corrosion current densities are expressed by $i^o{}_{corr}$ and i_{corr} in absence and presence of PGE, in that order.

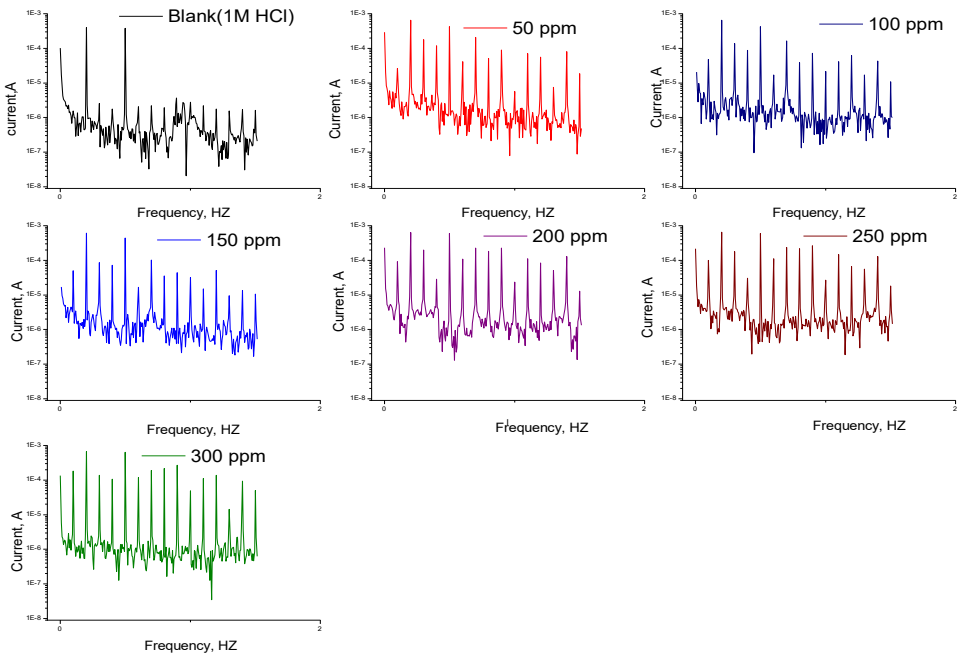

Figure 7: spectrums of Intermodulation for the corrosion of Al in 1 M HCl without and with different concentrations of PGE at 25˚C

Table 4: Electrochemical data gotten from EFM for Al in 1 M HCl without and with different concentrations of PGE

Inhibitor	[Inh] ppm	i_{corr} m A cm^{-2}	β_a mV dec^{-1}	β_c mV dec^{-1}	CF-2	CF-3	CRx10^3 mpy	Θ	IE%
Blank	0	1100	182	195	1.1	2.3	667	---	---
Punica Granatum extract	50	400.9	32	102	2.0	2.7	238	0.642	64.2
	100	348.8	31	66	1.1	2.9	207	0.688	68.8
	150	345.7	34	55	1.7	2.2	204	0.691	69.1
	200	342.8	24	36	1.8	2.5	146	0.694	69.4
	250	235.5	19	33	1.2	2.3	140	0.789	78.9
	300	214.3	18	25	2.0	2.3	127	0.809	80.9

3.**5. Adsorption Isotherm:** The application of adsorption isotherms was used for studying the interface degree among an inhibitor and Al surface[43, 44]. Θ represents the degree of surface coverage gotten from WL test and was measured as a function of inhibitor concentration in order to give the adsorption isotherms. Then we plotted the values of Θ to fit the most suitable adsorption model[45]. Different

isotherms contain Frumkin, Langmuir, Freundlich and Temkin isotherms were made to fit experimental value. The greatest fitted by Temkin isotherm as shown[46] in **Figure 8** .

$$\theta = {}^{2.303}/_{a}\ \log K_{ads} + {}^{2.303}/_{a}\ \log C \qquad (8)$$

The intercepts of Temkin are associated to the adsorption free energy ΔG^{o}_{ads} then we could obtain the K_{ads} use the following equation:

$$K_{ads} = {}^{1}/_{55.5}\ \exp\left({}^{-\Delta G^{o}_{ads}}/_{RT}\right) \qquad (9)$$

Where, 55.5 express the molar dose of water in solution in M^{-1}.

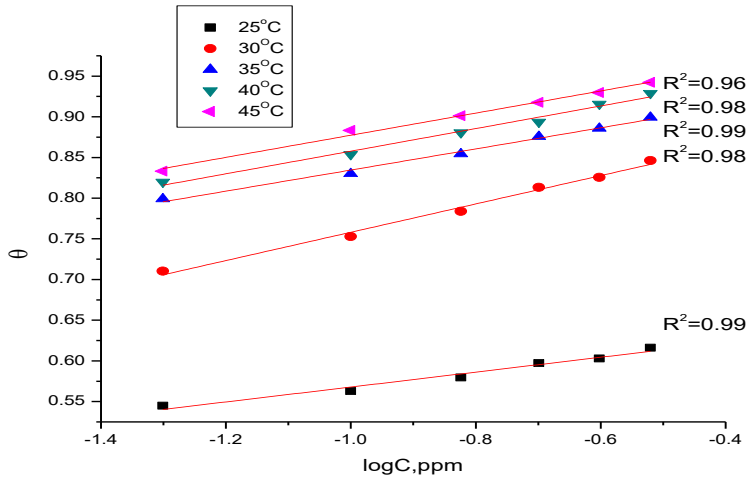

Figure 8: Temkin adsorption plots for Al in 1 M HCl containing PGE in various concentrations at 25°C

Plot of (ΔG^{o}_{ads}) Against T as in Figure 9 gave the (ΔH^{o}_{ads}) and (ΔS^{o}_{ads}) according to the equation 10:

$$\Delta G^{o}_{ads} = \Delta H^{o}_{ads} - T\,\Delta S^{o}_{ads} \qquad (10)$$

Table 5 obviously illustrates ΔG^{o}_{ads} excellent dependence on T, indicating the good correlation between thermodynamic data. The ΔG^{o}_{ads} negative sign data illustrate the spontaneity. Generally, ΔG^{o}_{ads} Values about -20 kJ/mol or lesser are corresponding to the electrostatic interaction among the charged plant extract and the charged Al (physisorption), but those around -40 kJ/mol or greater are conforming to the charge sharing or transfer from plant extract to the Al surface in order to form a coordinate kind of bond (chemisorption)[47]. The adsorption was found to be physical from the given data ofΔG^{o}_{ads} . Valuable information about the corrosion inhibition mechanism can be provided with the data for the adsorption of the inhibitor **(Table 5).** Endothermic adsorption procedure ($\Delta H^{o}_{ads} > 0$) is based clearly on chemisorption[48], an exothermic adsorption procedure ($\Delta H^{o}_{ads} < 0$) may contain either chemisorption or physisorption or a mixture of both procedures. The calculated ΔH^{o}_{ads} value in the present case for P.G.E adsorption in acidic solution indicating that, this inhibitor may be chemical adsorption. The ΔS^{o}_{ads} data in the inhibitors' existence are great and positive that has attended with endothermic procedure. This

designates that a lower in disorder occurred on profitable from reactions to the Al-adsorbed reaction complex[49].

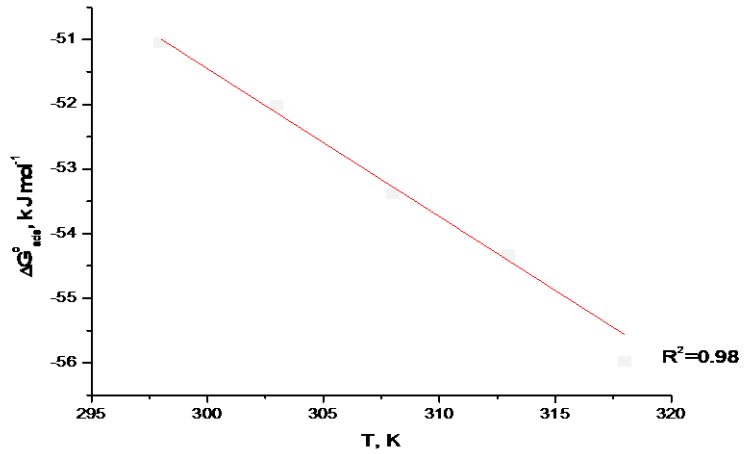

Figure 9: Variation of ΔG^o_{ads} vs T for PGE adsorption on Al surface in 1 M HCl at different temperatures

Table 5: Parameters of thermodynamic for the adsorption of PGE on Al in 1.0 M HCl at different temperatures

Inhibitor	Temp. °C	$K_{ads}x10^6$ M^{-1}	$-\Delta G^o_{ads}$ kJ mol^{-1}	ΔH^o_{ads} kJ mol^{-1}	ΔS^o_{ads} J mol^{-1} k^{-1}
Punica Granatum Extract	25	11.2	15.9	23.8	133.4
	30	14.8	16.9		134.4
	35	21.3	18.1		136.2
	40	25.2	18.9		136.3
	45	31.9	19.8		137.1

3.6 kinetic-thermodynamic corrosion parameters: At different temperatures (25-45ºC), weight loss method was accomplished in attendance of various doses of PGE It has been found that the corrosion rate is directly comparable to the temperature (table 1), which makes inhibition efficiency decreases with temperature. The corrosion parameter with and without PGE in the temperature range 25-45ºC has been summarized in **Table 1.** (E_a^*) which signifies the apparent activation energy for liquefied of Al in 1.0 M HCl was measured by using the Arrhenius equation from the slope of plots as following:

$$\log K = \frac{-E_a^*}{2.303\,RT} + \log A \qquad (11)$$

Where the rate of corrosion is expressed by K, E_a^* is the apparent activation energy and A is the Arrhenius pre-exponential factor.

The E_a^* values have been measured after getting the slope from plotting k_{corr} versus 1/T ($E_a^* = -\text{Slope x } 2.303 \text{ x R}$) **Figure 10.** E_a^* for the reaction of Al in 1 M HCl lower with of PGE (table 6). The formation of chemical bonds was strengthening as indicated from the decreasing in activation energy E_a^* by increasing temperature. However, extend of increasing in corrosion rate in the protected solution is lower than that in the solution of free acid. Thus, the protection efficiency of PGE rises noticeably with rising temperature. This result designates that the extract molecules adsorbed of on the Al surface may be chemical in nature. Thus, the adsorbed molecules number increases by increasing temperature leading to improve on protection efficiency. From the obtained results, PGE inhibits the corrosion by decreasing the reaction activation energy. This could be accomplished by adsorption of PGE molecules on the aluminum alloy surface, making a barrier for charge transfer[50]. Moreover, the great data of activation energy E_a^* with of PGE suggests a physical adsorption procedure occurrence. The entropy change (ΔS^*) and the enthalpy change (ΔH^*) both values can be calculated as follows:

$$K = \left(\frac{RT}{Nh}\right) exp\left(\frac{\Delta S^*}{R}\right) exp\left(\frac{\Delta H^*}{RT}\right) \qquad (12)$$

Where h expresses Planck's constant, k is a rate of corrosion, N is Avogadro number. A straight line should be given by plotting $\log {}^{k}/_{T}$ vs 1/T **(Figure 11),** with a slope of $(\Delta H^*/2.303R)$ and an intercept of $\left[\log(R/Nh) + \frac{\Delta S^*}{2.303R}\right]$, from which ΔS^* and ΔH^* data can be measured (table 6). The ΔS^* positive sign data for the inhibitor indicated that during the rate determining step, activated complex signifies dissociation rather than an association step, which mean improve in disorder occurs during the course of transition from the reaction to the activated complex[51]. The +ve sign ΔH^* indicated that the inhibitor molecule adsorption is an endothermic procedure.

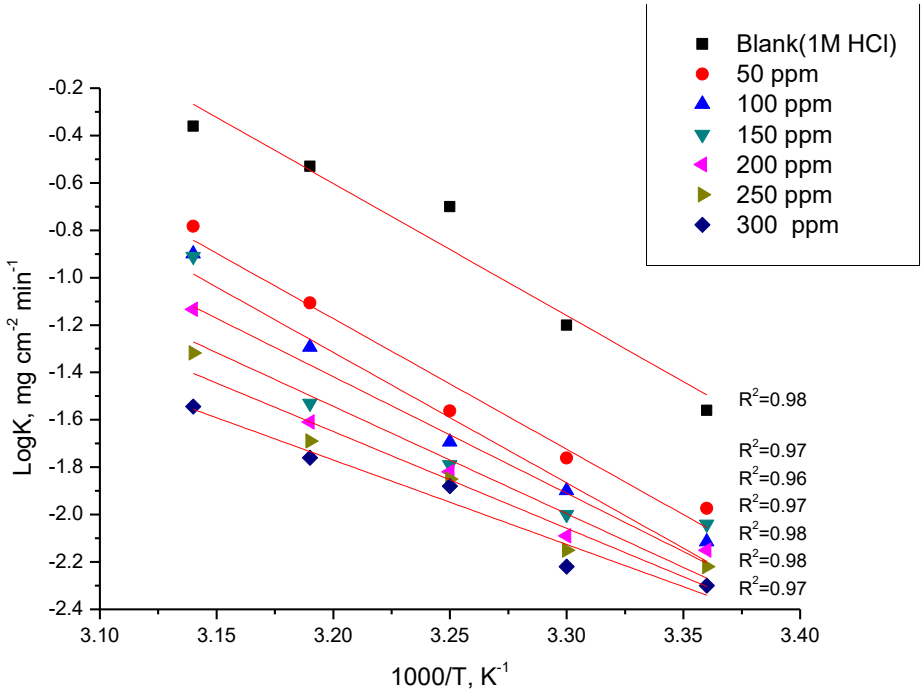

Figure 10: log k (corrosion rate) & 1/T curves for Al in 1 M HCl in the absence and presence of different concentrations of PGE after 60 min

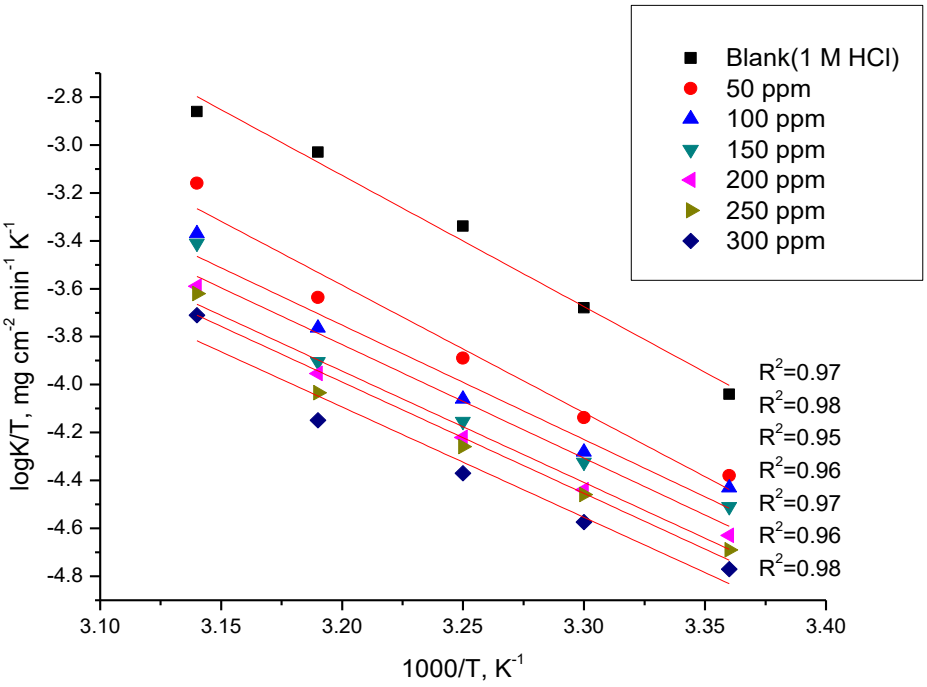

Figure 11: log *k*(corrosion rate)/T & 1/T curves for Al in 1 M HCl in the absence and presence of different concentrations of PGE after 60 min

Table 6: Activation parameters for Al dissolution in the attendance and lack of altered concentration of PGE in 1.0 M HCl after 60 min

Conc. Ppm	E_a^*, kJ mol^{-1}	ΔH^*, kJ mol^{-1}	ΔS^*, J mol^{-1}K^{-1}
1 M HCl	132.7	127.4	144.2
50	130.8	120.4	114.6
100	131.8	120.2	113.1
150	133.3	121.9	117.7
200	122.0	113.7	87.5
250	116.2	105.9	60.5
300	107.7	98.9	36.2

3.7 surface analysis by SEM**: Figure (11a)** illustrates the surface morphology of the polish Al electrode before being exposed to corrosion media (blank). The specimens were subjected to microscopic examination at x 2000. The micrograph shows a characteristic inclusion. SEM image was shown in **Figure (11b)** for the surface of the studied Al specimen after immersion for 24 hours in 1 M HCl solution. The micrograph illustrates a strong damage to the specimen surface. The corroded areas are shown as black grooves in specimen with gray and white zones, which correspond to the Al oxide dandruff. It suggested an uncovered surface of alloy electrode severally cored. The highly oxidized phase, perhaps formed in the air when dried up under no surface protection. Figure (11c) shows SEM images from the surface of another Al coin after inundation 1.0 M HCl solution for the same time interval in containing 300 ppm PGE. The micrograph illustrates that, the hindrance alloy surface is smoother than the unhindered surface, excellent protective film's existence on the Al surface. This approves that P.G.E is with the highest inhibition efficiency[52].

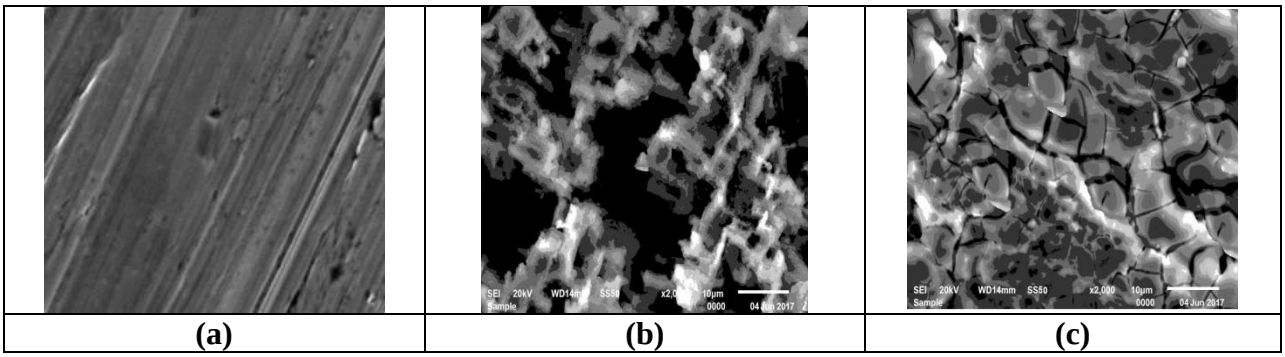

(a) **(b)** **(c)**

Figure 12: SEM Al surface micrographs (a) without immersion in 1 M HCl, (b) after 24 h of immersion in 1 M HCl and (C) after 24 h of immersion in 1 M HCl + 300 ppm of PGE at 25ºC

3.8 Corrosion inhibition mechanism: There is two kinds of interactions can illustrate the organic compound adsorption: chemisorption adsorption and physical. In general, both the electrically charged species in solution and charged Al surface are required in case of physical adsorption. The metal surface charge is in line for the electric field at the interface of the interface Al/solution. Otherwise, a chemisorption procedure includes charge transfer or charge sharing from the molecules of the inhibitor to the Al surface in order to form a coordinate kind of bond.

This is imaginable in both negative and positive surface charge. Normally, two kinds of inhibitor mechanisms were proposed. One was the creation of polymeric complexes with Al ions (Al^{+3}) rely on the real system[54,55]. The other was the chemical adsorption of PGE on Aluminum alloy surfaces[56,57]. The protective action of PGE does not happen by the simple blocking at the Aluminum alloy surface, exclusively at temperature greatly. This might be attributed to the various adsorption capacities of PGE on the Al surface at changed temperatures. It has been planned that by improving temperature, the effect of desorption of PGE on Al surface improves. Some of the hydrophilic groups with +ve sign atoms (O^{+}) desorbed from the surface of Al and did more work to stop H^{+} from getting nearby to the Al surface. So, at high temperature, PGE preferentially inhibited both anodic and cathodic corrosion processes[58].

CONCLUSIONS

The next conclusions can be deduced from the overall experimental results:

1. The PGE as corrosion protection for Al in 1 M HCl shows good performance.
2. The inhibiting action increases with the PGE concentration as shown from weight loss results and also increases with the increasing in temperature.
3. When PGE the addition takes place, a decreasing in double layer capacitances occurs unlike the blank solution. This confirms the PGE molecule adsorption on Al surface.
4. PGE inhibits the corrosion by being adsorbed on the Al surface according to the equation of the Temkin adsorption isotherm.
5. The obtained protection efficiencies by performing WL, EIS techniques and PP are all reasonably good matching.

REFERENCES

1. G.Trabanelli , *Corrosion*, 1991,47, 410.
2. D.N.Singh, A,K,Dey ., *Corrosion*, 1993,49, 594.
3. G.Banerjee, S,N,Malhotra , *Corrosion*, 1992,48, 10.
4. S.T.Arab, E.A.Noor , *Corrosion*, 1993,49, 122.
5. I.A.Raspini, Corrosion, 1993, 49,821.
6. Hari Kumar and S. Karthikeyan., *J. Mater. Environ. Sci. 2012*, 3 (5) 925–934.
7. Hadi Z.M. Al-Sawaad, Alaa S.K. Al-Mubarak, Athir M. HaddadI.,*J. Mater. Environ. Sci. 2010*, 1 (4), 227-238.
8. S.S.Abd El Rehim, H.Hassan, M.A. Amin, *Mater.Chem.Phys.*, 2003,78, 337.
9. R.F.V.Villamil, P. Corio, J.C.Rubim, M.L. SilivaAgostinho, *J. Electroanal. Chem.*, 1999,472, 112.
10. A.Khadraoui, A.Khelifa, Touafri L., Hamitouche H., Mehdaoui R., *J. Mater. Environ. Sci.* 2013, 4, 663.
11. M.Elachouri, M.S. Hajji, M. Salem, S. Kertit, R.Coudert, E.M.Essassi. *Corros.Sci*, 1995, 37, 381.
12. H.Luo, Y.C.Guan, K.N. Han , *Corrosion*,1998, 54, 619.
13. M.A.Migahed, E.M.S. Azzam , A.M. Al-Sabagh, *Mater. Chem.Phys*, 2004, 85, 273.
14. R.Guo,T. Liu, X.Wei, *Colloids Surf, A*, 2002,209, 37.
15. V.Branzoi, F. Golgovici, F.Branzoi, *Mater.Chem.Phys*, 2002, 78, 122.
16. K.S.Parikh,K.J. Joshi, *Trans. SAEST*, 2004,39, 29.
17. S.R.Al-Mhyawi, Orient Journal of Chemistry, 2014, 30, 3760.
18. A.I.Ali. and N. Foaud., J. Mater. Environ. Sci. 2012, 3 (5), 917-924.

19. O.F. Nwosu, E. Osarolube, L.A. Nnanna, C.S. Akoma, T. Chigbu, American Journal of Materials Science 4(4) (2014) 178-183.
20. A. O. James and O. Akaranta. African Journal of Pure and Applied Chemistry, 2009, 3(12), 262-268.
21. S.A.Graham, Thorne & Reveal, "Validation of subfamily names in Lythraceae". Taxon. Taxon, 1998, 47,. 2. 47 (2): 435–436.
22. Van Elswijk and others, 2004; Amakura and others, 2000; Seeram and others, 2005b..
23. B.A.Abd-El-Nabey , A.M. Abdel-Gaber, M., El. Said Ali , E.Khamis, S. El-Housseiny, *J. Electrochem. Sci*., 8(2013) 5851.
24. M.O.A.El Sheikh, G.M. El Hassan, A.H. El Tayeb, A.A. Abdallah, M.D. Antoun, Studies on Sudanese medicinal plants III: indigenous Hyoscyamusmuticus as possible commercial source for hyoscyamine. PlantaMedica, 1982, 45: 116–119.
25. M.Eeva, J.P. Salo, K.M. Oksman-Caldentey,,*J Pharm Biomed Anal*. 1998, 16(5):717. "Determination of the main tropane alkaloids from transformed Hyoscyamusmuticus plants by capillary zone electrophoresis".
26. G.N.Mu, T.P. Zhao, M. Liu T. Gu, *Corrosion*, 1996, 52, 853.
27. R.G.Parr, R.A. Donnelly, M. Levy, W, E. Palke, *J. Chem. Phys*., 1978,68, 3801.
28. R.W.Bosch, J. Hubrecht, W.F. Bogaerts, B.C. Syrett , *Corrosion*,2001, 57, 60.
29. D.Q.Zhang, Q.R.Cai,X.M.He ,L.X. Gao, G.S.Kim ,*Mater. Chem. Phys*. 2009,114, 612.
30. H.P.Lee, K. Nobe, *J. Electrochem. Soc*.1986, 133, 2035.
31. Tao Z. H., Zhang S. T., Li W. H., Hou B. R.,*Corros. Sci*. 2009,51,2588.
32. Ferreira E. S.,Giacomelli C., Giacomelli, F. C., Spinelli A.,*Mater. Chem.Phys*.2004, 83, 129.
33. Paskossy T., *J. Electroanal. Chem*, 1994, 364, 111.
34. Growcock F. B.,Jasinski J. H., *J. Electrochem. Soc*., 1989,136, 2310.
35. Abd El-Rehim S. S., Khaled K. F.,Abd El-Shafi N. S.,*Electrochim. Acta*, 2006, 51, 3269.
36. M.Metikos , R.Hukovic,Z. Bobic, S. Gwabac,*J. Appl. Elactrochem*., 1994,24, 772.
37. A.Caprani,I. Epelboin,Ph. Morel, Takenouti H.,*proceedings of the 4th European sym. on Corros. Inhibitors*, 1975,571.
38. J.Bessone,C. Mayer, K. Tuttner, W.Lorenz, J.,*Electrochim. Acta*, 1983, 28, 171.
39. I.Epelboin,M. Keddam,H. Takenouti , *J. Appl. Electrochem*.,1972, 2, 71.
40. Benedeti A. V.,Sumodjo P. T. A., Nobe K., Cabot P. L., Proud W. G.,*ElectrochimicaActa*, 40 (1995) 2657.
41. H.Ma, S. Chen, L.Niu, S. Zhao, S. Li, D. Li, *J. Appl. Electrochem.* 32 (2002) 65.
42. X.H.Li, S.D.Deng, H. Fu,,*J. Appl. Electrochem*., 40 (2010) 1641.

43. M.Lagrenee, B. Mernari, M. Bouanis, M. Traisnel, F. Bentiss, Corros. *Sci*., 2002, 44, 573.
44. E.Kus, F. Mansfeld, *Corros. Sci*., 2006, 48, 965.
45. G.A.Caigman, S.K. Metcalf, E.M. Holt, *J.Chem. Cryst*, 2000, 30, 415.
46. S.S.Abdel–Rehim, K.F. Khaled, N.S. Abd–Elshafi, *Electrochim. Acta*, 2006,51,3269.
47. J.O.BockrisD.A.J. Swinkels, *J. Electrochem. Soc*., 1964,111,736.
48. W.J.Lorenz, F. Mansfeld, Corros. *Sci., 1981*, 21,647.
49. A.Yurt, G.Bereket ,A. Kivrak ,A. Balaban, & B.Erk B, *J Appl Electrochem*, 2005,35 , 1025.
50. F.Bentiss,M. Traisnel,M & Lagrenee M, *Corros Sci.,2000,* 42 , 127.
51. M.M.Saleh, A.A. Atia, *J. Appl. Electrochem*., 2006, 36, 899.
52. L.Narvez, E.Cano,D.M. Bastidas, *J. Appl. Electrochem*., 2005,35, 499.
53. X.H.Li, S.D. Deng, H. Fu, Corros. *Sci*., 2009, 51, 1344.
54. I.K.Putilova, S.A. Balezin, Y.P. Barasanik,*Metallic Corrosion Inhibitors*, *Oxford: Pergamon Press*, 1960, 30.
55. V.R.Saliyan, A.V. Adhikari, *Bull. Mater. Sci*., 2007, 31, 699.
56. Y.Li, P. Zhao, Q. Liang, B.Hou, *Appl. Surf. Sci*., 2005, 252, 1245.
57. A.H.Mehaute , G.Grepy ,*Solid State Ionics*,1989, 9–10, 17.
58. V.Brusic, M.A.Frisch, B.N.Eldridge,F.P. Novak, F. B. Kauman , B.M.Rush, G.S.Frankel,,*J. Electrochem. Soc*. 1991, 138, 2253.

Corresponding author: A.S.Fouda

Department of Chemistry, Faculty of Science, Mansoura University, Mansoura

Egypt, Email: asfouda@hotmail.com

Online publication Date: 11.05.20187